The *Drosophila abrupt* gene encodes a BTB–zinc finger regulatory protein that controls the specificity of neuromuscular connections

Song Hu,[1,3,5] Douglas Fambrough,[4,5] Julie R. Atashi,[1,2] Corey S. Goodman,[4] and Stephen T. Crews[1,2,6]

[1]Department of Biochemistry and Biophysics and [2]Curriculum in Neurobiology, School of Medicine, The University of North Carolina at Chapel Hill, Chapel Hill, North Carolina 27599-7260 USA; [3]Department of Biology, University of California at Los Angeles, Los Angeles, California 90024 USA; [4]Department of Molecular and Cell Biology, Howard Hughes Medical Institute, University of California at Berkeley, Berkeley, California 94720 USA

Motor axons make synaptic connections with specific muscles, and this specificity unfolds during development as motoneuron growth cones make specific pathway choices and ultimately recognize and synapse on their specific muscle targets. The *Drosophila clueless* mutation was identified previously in a genetic screen for mutations that disrupt motoneuron guidance and connectivity. We show here that *clueless* is allelic to *abrupt*. The *abrupt* gene is required for the embryonic formation of specific synaptic connections between a subset of motoneurons and a subset of muscles. Mutations in *abrupt* also reveal its role in establishing and maintaining muscle attachments, adult sensory cell formation, and morphogenesis of adult appendages. The *abrupt* gene encodes a zinc finger protein with a conserved BTB domain. *abrupt* is expressed in muscle nuclei but not motoneurons, suggesting that *abrupt* controls the muscle expression of molecules required for correct motoneuron targeting, as well as molecules required for correct muscle attachments.

[*Key Words*: *abrupt*; *Drosophila*; neuromuscular connections; muscle; transcription factor; zinc finger]

Received August 3, 1995; revised version accepted October 20, 1995.

Coordinated movement requires that muscles be properly innervated by the appropriate motoneurons. The specificity of neuromuscular connections unfolds during embryonic development as motoneuron growth cones extend into peripheral tissues, make a series of pathway choices that lead them into the correct region of mesoderm, and ultimately recognize and synapse onto their appropriate muscle targets. The *Drosophila* embryo provides a simple and convenient system for genetically dissecting the molecular mechanisms that control neuromuscular connectivity. In each A2–A7 abdominal hemisegment of a *Drosophila* embryo, ~50 motoneurons (H. Sink and R. Fetter, pers. comm.) innervate 30 individually identified muscles in a highly specific and stereotypic manner (Johansen et al. 1989a,b; Halpern et al. 1991; Sink and Whitington 1991). Evidence for specificity among connections is further revealed by experimental manipulations in which the number or positions of muscles are altered (for review, see Keshishian et al. 1993). These observations suggest a model in which specific synaptic connections between motoneurons and muscles in *Drosophila* are determined by surface and/or secreted recognition molecules expressed by muscles.

Muscle development occurs in a series of events (Bate 1990, 1993). Mesoderm-derived myoblasts proliferate during embryonic stage 14, giving rise to muscle pioneers (founder cells), which prefigure the position and patterning of somatic muscles. Additional myoblasts fuse with the founder cells to form a muscle syncitium. Muscle fibers extend toward and attach to the underlying epidermis at stage 16. The muscles are innervated by motoneurons during stage 16. Each of the 30 individual muscle fibers in each abdominal segment (A2–A7) has a unique position, morphology, pair of attachment sites, and motoneuron innervation.

During development, the embryonic muscles are innervated by motoneurons that exit the central nervous system (CNS) in two main pathways: the segmental nerve (SN) and the intersegmental nerve (ISN) (Johansen et al. 1989a, 1989b; Sink and Whitington 1991). The ISN represents a single major nerve branch, whereas the SN splits into four branches: SNa, SNb, SNc, and SNd. The ISN innervates dorsal muscles, SNa projects to lateral muscles, SNb innervates ventrolateral muscles, and SNc and SNd project to the most ventral muscles. Of partic-

[5]The first two authors contributed equally.
[6]Corresponding author.

ular interest are four motoneurons: RP1, RP3, RP4, and RP5. Their cell bodies lie adjacent to each other near the midline of the CNS. Their axons fasciculate together, extend across the midline, and exit the contralateral side of the CNS. They extend out via the ISN and then leave the ISN in the SNb, where they enter and explore the ventral muscle region. The growth cones of these motoneurons form a stereotyped three-branched terminal arbor as they make specific synaptic connections onto ventral muscles 7 and 6 (RP3), 13 (RP1, RP4), and 12 (RP5). Other SNb motoneurons innervate these same muscles.

We would expect that the ability of individual motoneurons to recognize specific muscles requires the interactions between receptor molecules on the motoneuron growth cones with recognition molecules either secreted or localized on the surface of muscle targets. The identity of the regulatory, signaling, receptor, and downstream molecules that control this specificity of connections is largely unknown. However, a number of surface and secreted molecules have recently been implicated in playing a role in these events in *Drosophila*, including Connectin (Nose et al. 1994), Fasciclin III (Chiba et al. 1995), and Semaphorin II (Matthes et al. 1995).

Regulation of the identity of certain muscles in *Drosophila* is under the control of the homeo box-containing proteins *S59* and *apterous* (Dohrmann et al. 1990; Bourgouin et al. 1992). It is not known whether these types of muscle identity genes on their own control the expression of specific surface and/or secreted muscle recognition molecules or, alternatively, whether other regulatory genes are interposed lower in the hierarchy to control the expression of these recognition molecules. In this paper we present evidence showing that a more ubiquitously expressed muscle regulatory gene, *abrupt* (*ab*), may be required for the expression of the surface and/or secreted muscle identifiers that allow the SNb motoneurons to recognize their specific ventral muscle targets.

Identification of molecules that mediate neuromuscular connectivity has been achieved by two main approaches. The first approach involves identifying genes by their patterns of expression, using either monoclonal antibody screens (e.g., Fasciclin III, Patel et al. 1987; Semaphorin II, Kolodkin et al. 1992) or enhancer trap screens (e.g., Connectin, Nose et al. 1992). Although none of these three genes have striking loss-of-function mutant phenotypes in this system, all three display striking neuromuscular phenotypes in gain-of-function conditions when the genes are ectopically expressed (Nose et al. 1992, 1994; Chiba et al. 1995; Matthes et al. 1995). The second approach involves identifying genes by their mutant phenotypes (Van Vactor et al. 1993). The initial mutant screen focused on the second chromosome and identified three genes affecting axon guidance (*beaten path*, *short stop*, and *stranded*) and two genes affecting neuromuscular connectivity [*clueless* (*clu*) and *walkabout* (*wako*)].

The *clu* and *wako* genes show similar mutant phenotypes that affect only a subset of motoneuron connections: The SNb motoneurons fail to form their normal synapses on the ventral longitudinal muscles. In clu^1 mutant embryos, the SNb makes correct pathway choices and reaches the ventral muscle field. However, it fails to establish its typical three-branch terminal arbor morphology, and instead, the growth cones wander and terminate at ectopic locations. Target muscle recognition of neighboring nerve branches are unaffected in clu^1 mutant embryos, as both the ISN and SNa form appropriate synapses. Thus, *clu* is not required for synaptogenesis in general but, rather, appears to control the ability of a group of motoneurons to identify their specific targets from within a group of neighboring muscles.

In this paper we show that *clu* is allelic to the *Drosophila ab* gene and that null mutations of *ab* display a motoneuron targeting defect similar to that described previously for the ethylmethane sulfonate (EMS)-induced clu^1 mutation. We also describe additional defects in embryonic muscle attachment and in postembryonic morphology. Molecular analysis of the *ab* gene indicates that it encodes a zinc finger (ZF) transcription factor containing a conserved BTB domain. *ab* is expressed in the nuclei of muscles but not motoneurons, suggesting that *ab* controls muscle-specific gene expression required for target recognition by appropriate motoneurons.

Results

Two enhancer trap insertions identify the ab *gene*

Enhancer trap lines representing 1500 distinct *P[lacZ]* insertions were screened for expression of β-galactosidase in the embryonic CNS midline cells (Crews et al. 1992). The BL97 line showed strong embryonic CNS midline staining as well as epidermal and imaginal disc expression. The insertion was mapped by polytene chromosome in situ hybridization to chromosomal interval 32E1-2. The laboratories of Jose Campos-Ortega (University of Cologne, Germany) and Elisabeth Knust also identified an enhancer trap insertion (94) at 32E that revealed a similar pattern of expression and thus was likely to be an insertion in the same gene.

The *ab* gene discovered by Bridges and colleagues around 1925 is located at 32E. Mutations in the ab^1 allele are characterized by the failure of longitudinal wing vein L5 to extend to the wing margin (Fig. 1a,b; Lindsley and Zimm 1992). The BL97 line is homozygous viable and has a wild-type wing venation pattern. However, the homozygous 94 line reveals an L5 wing venation defect similar to *ab* (Fig. 1C). The 94 insertion line fails to complement *ab*, indicating that the 94 line has an *ab* mutation (Fig. 1D). When the P element is excised by the introduction of transposase, the 94 wing defect reverts to wild type in multiple lines, indicating that the P-element insertion is the cause of the wing defect. These results suggested that the 94 insertion disrupts the *ab* gene and that the BL97 insertion may be adjacent to the *ab* gene.

clu *is allelic to* ab

The original *clu* mutation (clu^1) originated from an EMS

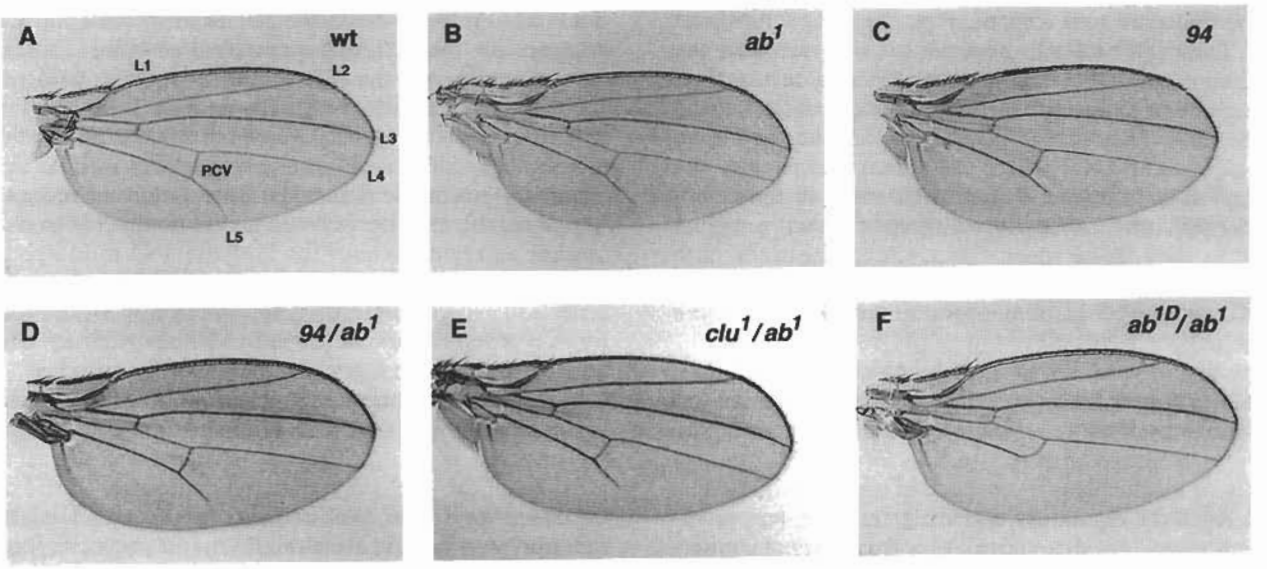

Figure 1. The 94 P-element insertion and *clu* are alleles of *ab*. (*A*) Wild-type (wt) adult wing. Conspicuous are the five longitudinal wing veins, designated L1–L5, and the PCV. Notice that L5 extends continuously from the PCV to the wing margin. (*B*) ab^1 wing venation defect. Veins of ab^1 homozygous individuals show loss of L5 between the margin and PCV. Other veins are similar to wild type. (*C*) 94 P-element insertion wing venation defect. Veins of 94 homozygous individuals show loss of L5 between the margin and PCV similar to ab^1 homozygotes. (*D*) Transheterozygotes of 94 and ab^1 fail to complement, revealing an L5 wing defect. (*E*) Transheterozygotes of the lethal clu^1 mutation and ab^1 fail to complement, showing an L5 wing defect. (*F*) Transheterozygotes of ab^1 and ab^{1D} show a more severe wing venation defect resulting in a complete absence of L5 between the PCV and margin.

screen for mutations that disrupt motoneuron guidance and connectivity (Van Vactor et al. 1993). The clu^1 mutation shows normal motor axon pathfinding but defective connectivity of the SNb motoneurons with their synaptic muscle targets. Genetic mapping placed the clu^1 mutation in the 32E region. The clu^1 allele fails to complement ab^1 and shows the L5 wing venation defect (Fig. 1E). This indicates that *clu* is allelic to *ab* (clu^1 is redesignated ab^{clu1}). Two additional EMS alleles (ab^{clu2} and ab^{clu3}) were identified in a screen for noncomplementation of clu^1 lethality, and several X-ray-induced alleles were identified in a screen for noncomplementation of the *ab* adult phenotype. The heteroallelic combinations of these new alleles indicate that *ab* is a lethal locus.

ab *null mutations show motoneuron connectivity defects*

Further genetic analysis of *ab* required the generation of null mutations. No preexisting deficiencies uncovered the 32E region, so we utilized both P-element transposase-induced excision/local-hopping and γ-ray mutagenesis to create chromosomal deletions that remove *ab*. Both ab^{1D} and ab^{G5} were found to be amorphic on the basis of genetic and molecular analysis (see below; Fig. 3). It is likely that ab^{1D} represents a null mutation specific for *ab*, whereas ab^{G5} may uncover additional, unidentified genes.

Previous work on ab^{clu1} (Van Vactor et al. 1993) revealed a specific motoneuron connectivity defect in which SNb motoneurons fail to make proper synaptic connections with their ventral longitudinal muscle targets. Utilizing the new *ab* alleles, the *ab* connectivity defect was further investigated using monoclonal antibody (mAb) 1D4 that stains all motor axons and terminal arbors, and mAb 2D5 that recognizes Fasciclin III and stains the RP neurons. The ab^{1D} and ab^{G5} null alleles and the three ab^{clu} alleles were analyzed as homozygotes and as heterozygotes over ab^{G5}. Staining with mAb 2D5 indicates that the RP neurons form and are located at their normal positions within the CNS. In addition, staining with mAb 1D4 shows that their axons make the appropriate pathway choices to reach the ventral muscle field. However, in *ab* mutant embryos, the SNb axons pause at the proximal edge of muscle 13 and form abnormal branches instead of forming their wild-type axonal extensions onto the muscle fibers. These aberrant branches wander over the prospective target muscles and occasionally form connections at ectopic sites, such as at or near muscle 8. At embryonic stage 17, *ab* mutants do not establish the normal three-branched terminal arbor of SNb axons on muscles 7, 6, 13, and 12 (Fig. 2A–C). The transverse nerve is often incomplete and invades the ventral muscle field. Ectopic endings from the transverse nerve are seen in other mutations that disrupt SNb innervation of the ventral muscles (D. Fambrough, D. Van Vactor, H. Sink, C. Kopczynski, and C.S. Goodman, unpubl.).

The targeting defects in *clu* mutants are limited to the ventral region of the embryo; the connectivity of the motor axons in the ISN and SNa is normal. The SNc and,

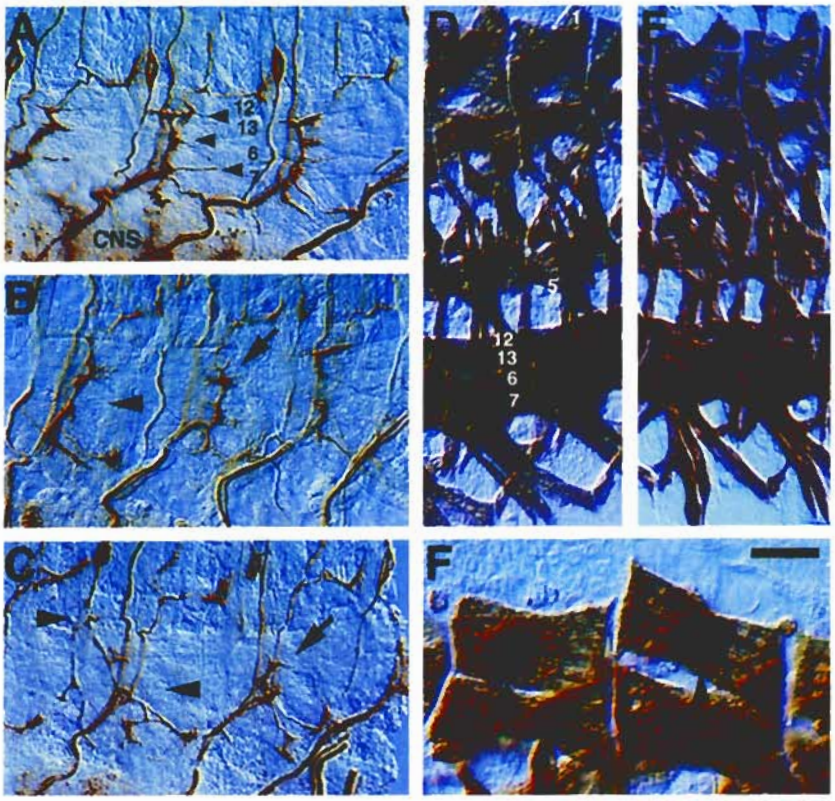

Figure 2. Mutations in *ab* result in SNb connectivity and muscle attachment defects. (*A–C*) Three abdominal segments stained with mAb 1D4 and HRP–DAB histochemistry to visualize motoneurons. (*D–F*) Two abdominal segments stained with anti-myosin and HRP–DAB histochemistry to visualize muscles. In all panels, dorsal is up and anterior is *left*. The embryos are late stage 16, except *F* that shows a mid-17 stage embryo. (*A*) A wild-type embryo showing the stereotypic three-branch terminal arbor of the SNb (arrowheads). Muscles 7, 6, 13, and 12 and the CNS are labeled for reference. (*B*) An ab^{clu1} homozygous embryo showing SNb connectivity defects. Muscles 7 and 6 are not innervated (arrowhead), and SNb axons have stalled while exploring the proximal edge of muscle 13 (arrow). (*C*) An ab^{1D} homozygous embryo showing similar SNb connectivity defects. The SNb makes an ectopic connection at the transverse nerve (*left* arrowhead) while failing to innervate muscles 7 and 6 (*right* arrowhead). Another SNb has stalled prematurely (arrow). (*D*) A wild-type embryo showing the normal muscle pattern. Muscles 1, 5, 6, 7, 12, and 13 are labeled. (*E*) An ab^{1D} embryo showing that the muscle pattern is relatively normal in *ab* null mutants. An exception is the occasional misinsertion of lateral longitudinal muscles. In this embryo, muscle 5 has inserted in an ectopic location (arrowhead). (*F*) Muscle 1 pulls out of its insertion sites following the onset of muscle contractions. This ab^{1D} embryo, which is older than the embryos shown in *D* and *E*, has two segments where muscle 1 lost attachment and formed a ball of muscle tissue (arrowheads). Scale bar, (*A–C*) 20 μm, (*D–E*) 30 μm, (*F*) 16 μm.

rarely, SNd show some morphological abnormality, but the small size and deep ventral position of these nerve branches make their connectivity more difficult to assess. All alleles and allelic combinations described here show similar defects to each other and to those observed previously for ab^{clu1}. However, weak adult viable alleles, such as ab^{1}, do not show motoneuron connectivity defects.

ab *null mutations show muscle attachment defects*

Analysis of the mature embryonic muscle pattern in *ab* mutants reveals that most muscles appear normal in their position, number, morphology, and expression of Muscle Myosin, which is expressed in all muscles, and Fasciclin III and Connectin, which are expressed on the surface of subsets of muscles.

However, a few muscles show variably penetrant defects in their attachment to the epidermis. Some of the lateral longitudinal muscles (3, 5, 11, and 20) also show variably penetrant defects in the locations of their muscle attachments (Fig. 2E). It should be noted that the muscles in which we observe the connectivity defect (7, 6, 13, and 12) are distinct from the muscles in which we observe the attachment site defect (3, 5, 11, and 20).

In addition, several muscles that initially attach at the proper locations by stage 16, at later stages (after innervation and muscle contraction have begun) display spheroid phenotypes in which the muscles pull out of their insertion sites and round up into spheres. This is seen most commonly with muscle 1 and, to a lesser extent, with muscle 2, although in both cases it is highly variable (Fig. 2F). This phenotype could be owing to either a muscle or an epidermal defect that impinges on the strength and quality of the muscle insertions. The defect is observed in most strong *ab* alleles (ab^{1D}, ab^{G5}, ab^{clu2}, and ab^{clu3}), although expressivity is low with only a few hemisegments in an embryo affected. Weak alleles such as ab^{1} do not show either muscle phenotype. Interestingly, the ab^{clu1} mutation does not show the spheroidal muscle defect; ab^{clu1} does show the incorrect muscle attachment site defect, although at a weaker penetrance than in the stronger alleles. The absence of the spheroid phenotype in ab^{clu1} may be attributable to the nature of the molecular lesion in this allele, which results in a truncated protein lacking the ZF DNA-binding domain (see below).

Adult phenotypes of ab *mutants*

Examination of viable (weak) *ab* alleles and viable combinations of lethal (strong) *ab* alleles over viable alleles

reveals that *ab* function is required for the development of numerous adult structures. For example, ab^1 and *P[94]* are recessive viable mutations that show wing venation and macrochaete (bristle) defects. More severe defects can be seen in combinations of other alleles. Combining the two pupal lethal mutations, ab^{60M} (a P-element excision derivative of *P[BL97]*) and ab^{G9} (γ-ray allele from *P[94]*), results in adult escapers that display a broad range of defects. Similar defects are also observed in combinations of a viable allele (ab^1, *P[94]*) with a lethal allele (ab^{1D}, ab^{G5}, and ab^{clu3}).

Wing venation and bristle defects in ab^{60M}/ab^{G9} and ab^1/ab^{1D} adult flies show more severe defects than observed with ab^1 and *P[94]*. The wing veins are completely absent between the margin and posterior crossvein (PCV) (Fig. 1F), in contrast to ab^1 and *P[94]* homozygotes and heterozygotes, which are missing only a smaller section of L5 (Fig. 1B–D). There is also a more severe loss of the thoracic and wing mechanosensory bristles in the transheterozygote combinations. Two posterior scutellar bristles and two upper humeral bristles are invariably missing, and the super-alar bristles are usually fewer in number than wild type. Occasionally, one of the campaniform sense organs on wing vein L3 is absent.

In addition, legs of ab^{60M}/ab^{G9} flies are severely gnarled, and the more distal segments are shortened in length or absent. The antennal aristae are also deformed, and there is a furrow at the midline of the dorsal thorax with polarity altered of the remaining bristles. Males of ab^{60M}/ab^{G9} and ab^1/ab^{1D} genotypes are sterile, and their external genitalia are rotated 180° relative to wild type. Many of these additional phenotypes are described for the ab^2 allele (Lindsley and Zimm 1992). This broad range of phenotypes indicates that *ab* is involved in multiple developmental processes.

The fact that ab^1/ab^{1D} displays stronger and additional defects as compared with ab^1 itself suggests that *ab* function is dosage dependent. Both penetrance and expressivity of wing venation and bristle defects correlate with the following allelic strength: $ab^1/ab^1 = P[94]/P[94] < ab^1/ab^{60M} = ab^1/ab^{G9} < ab^1/ab^{1D} = ab^1/ab^{G5}$. Less than 20% of homozygous *P[94]* and ab^1 flies exhibit phenotypes, and the phenotypes are weak. Fifty percent of ab^1/ab^{60M} flies display an intermediate phenotype. One hundred percent of ab^1/ab^{1D} flies have severe defects. In addition, ab^1/ab^{1D} displays leg and antennal defects that are not observed in ab^1 alone. One simple explanation is that *ab* functions in a concentration-dependent manner, with each process requiring a threshold level of *ab* expression.

Molecular cloning of the ab *locus*

Molecular cloning of the *ab* gene was initiated using inverse PCR to clone the genomic DNA adjacent to the *P[BL97]* insertion. Genomic DNA representing 33-kb was isolated by screening a wild-type genomic clone library followed by chromosomal walking (Fig. 3). Restriction fragments covering the entire DNA interval were hybridized in situ to whole-mount embryos to identify the *ab* transcription unit. The presence of a transcription unit was found adjacent to the *P[94]* insertion (probe d) and extends to the end of the walk (probes e–k; >21 kb).

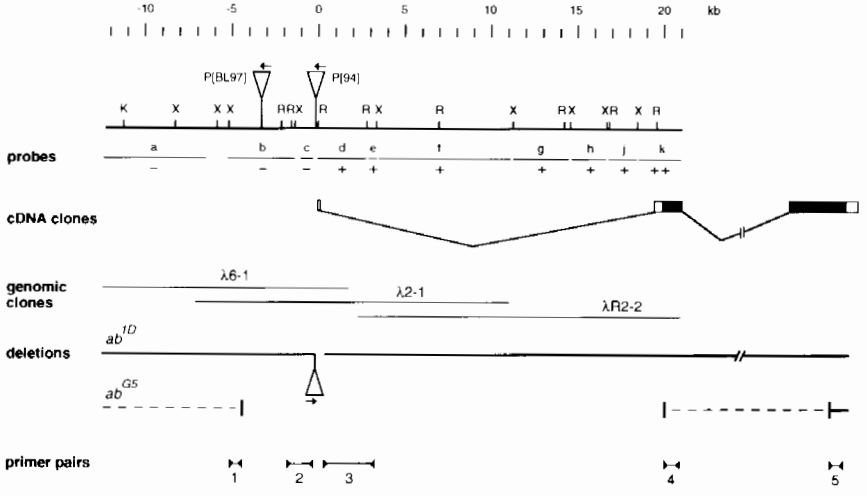

Figure 3. Structure of the *ab* gene. The extent of the *ab* gene chromosomal walk is shown as a 33-kb DNA interval. The scale is marked with 1-kb intervals, and the location marked "0" denotes the 5′ end of the longest cDNA clone. Numbers increase in the 5′ to 3′ direction with respect to *ab* cDNA sequences. Below the scale is the restriction enzyme map for the enzymes: *Eco*RI (R), *Kpn*I (K), and *Xba*I (X). The positions of the BL97 and 94 P-element insertions are indicated by the vertical lines extending from the inverted triangles, and direction of *lacZ* transcription is indicated by arrows. Fragments used for whole-mount embryonic in situ hybridization experiments are listed in alphabetical order below the restriction map. The presence (+) or absence (−) of hybridization is shown. Probes a–c failed to detect embryonic transcription, whereas probes d–k revealed the same embryonic expression pattern. Probe k was particularly intense (++) and was used to isolate *ab* cDNA clones. The extent of the pcab cDNA clones is illustrated. (□) Untranslated regions; (■) coding sequence. The 3′ sequences are located outside the cloned genomic region, and thus, the intron–exon structure of the gene is incomplete. Genomic clones λ6-1, λ2-1, and λR2-2, which define the walk, are shown. The location and extent of two deletion mutants were mapped by single-embryo PCR and Southern blot analysis. The locations of the primer pairs used for PCR are shown at *bottom*. The ab^{1D} excision mutation of *P[94]* contains an 0.7-kb deletion removing exon 1. The P-element has reinserted in the opposite orientation to *P[94]*. The ab^{G5} γ-ray mutation is absent for all primer pairs except pair 5. This indicates that the rightward extent of the deficiency lies within the *ab* transcription unit (broken line between vertical lines), but the leftward extent of the deletion is unknown (broken line). Thus, additional genes may be absent in ab^{G5}.

The embryonic expression pattern of this transcript is identical to the *lacZ* expression pattern from the BL97 and 94 enhancer trap lines. Fragments upstream of the *P[94]* insertion failed to detect embryonic transcripts by whole-mount in situ hybridization or Northern analysis. Thus, no other detectable embryonic transcript lies within the 12 kb of the identified transcription unit. Sequence and breakpoint analyses of mutant alleles (see below) show that this is the correct transcript.

Using a probe derived from fragment k that gave the strongest signal by in situ hybridization, multiple cDNA clones were isolated. Northern analysis with a fragment common to all cDNA clones revealed a single 5.1-kb transcript. The longest cDNA clone we isolated is 5 kb and thus near full length. Sequence and Southern blot hybridization analyses of both cDNA and genomic clone DNA placed the 5′ end of the longest cDNA clone 141 bp downstream from the *P[94]* insertion site and 3.3 kb away from the P[BL97] insertion site. Genomic DNA containing the 3′ end of the *ab* gene was not cloned.

Temporal and spatial expression of ab

We determined the pattern of *ab* expression using three different methods, all of which yielded similar results: in situ hybridization with *ab* cDNA probes, staining with a rat polyclonal Ab antisera, and anti-β-galactosidase staining of the *ab* enhancer trap lines. The specificity of the polyclonal Ab antisera was confirmed by absence of staining in ab^{1D} null mutant embryos (Fig. 4F). In all tissues in which it is expressed, the Ab antisera indicates that the Ab protein is expressed in the nucleus.

Nervous system expression

Initial *ab* expression is within the CNS midline cells (Fig. 4A–C). Beginning at stage 9, uniform CNS midline precursor staining is observed and expression continues in these cells through stage 13. Stained cells include the precursors to the VUM cells, some of which contribute axons to the SNb. Importantly, the CNS midline cells are the only embryonic CNS cells to express *ab*. Neither the lateral neuroectodermal precursor cells nor mature lateral CNS neurons express *ab*. In particular, the RP1, RP3, RP4, and RP5 motoneurons, whose muscle connectivity is affected in *ab* mutant embryos, do not express detectable levels of *ab* as assessed by in situ hybridization, *lacZ*, and anti-Ab staining (Fig. 4C). Additional nervous system expression is observed in the precursors and mature cells that constitute the stomagastric nervous system.

Epidermal expression

Segmentally repeated stripes of ectodermal expression appear at stage 11 (Fig. 4A), and the expression becomes uniform throughout the entire epidermis by stage 12 (Fig. 4E) with the exception of the tracheal cells where it is absent. Strong epidermal expression continues throughout embryogenesis and is uniform except for stronger expression in the specialized segmental border cells.

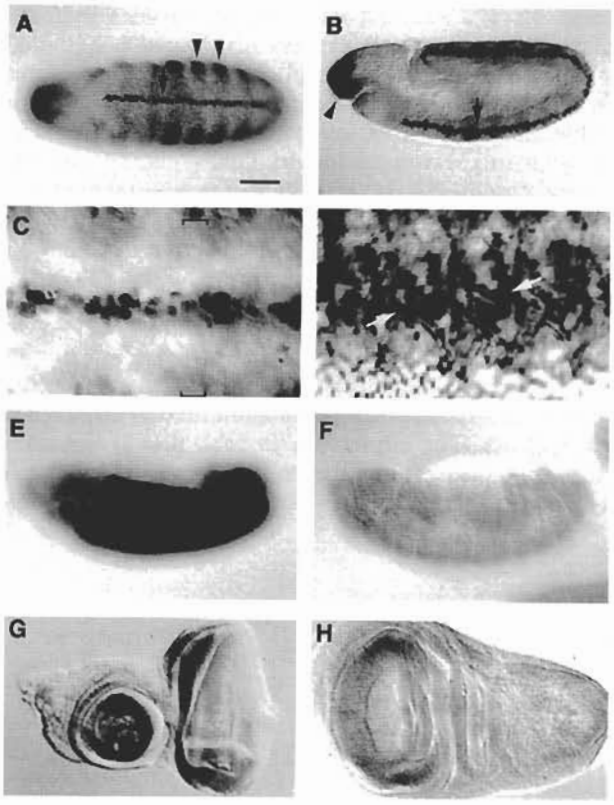

Figure 4. Embryonic and imaginal expression of *ab*. (*A*) Ventral view of stage 11 embryo stained with Ab antisera shows strong CNS midline precursor staining (arrow) and segmentally repeated ectodermal stripes (arrowheads). Anterior is at *left* in this and subsequent panels. (*B*) Sagittal view of stage 11 embryo stained with Ab antisera indicating CNS midline precursor (arrow) and stomagastric nervous system precursor cell (arrowhead) expression. (*C*) High-magnification view of the CNS of a stage 14 dissected embryo showing CNS midline expression of Ab and absence of Ab expression in lateral CNS. The BL97 line was stained with anti-β-galactosidase; identical results were obtained by staining with the Ab antisera and in situ hybridization with an *ab* cDNA probe. Shown are three ganglia, and the bracket indicates the lateral borders of the CNS. (*D*) Nuclear Ab expression in syncytial muscle fibers. Prominently shown are the ventral muscles in a filleted stage 17 embryo. The epidermal staining in the background obscures the muscle staining. However, it is apparent that all muscles express Ab including muscles 7, 6, 13, and 12 that show connectivity defects in *ab* mutants. Arrows indicate nuclear staining within muscles 7 and 6; muscles 13 and 12 are not in focus in this photograph. (*E*) Uniform epidermal expression shown in a sagital view of a stage 13 embryo stained with Ab antibody. (*F*) Absence of Ab antibody expression in homozygous ab^{1D} mutant stage 13 embryo. (*G*) X-gal staining of eye–antennal disc from the BL97 line. Expression is widely distributed throughout the disc. (*H*) The wing–notum disc of BL97 shows widespread expression of *lacZ* as assayed by X-gal staining. Scale bar, 70 μm (*A*, *B*, *E*, *F*), 18 μm (*C*), 30 μm (*D*), and 75 μm (*G*, *H*).

Muscle expression

During myoblast fusion and syncytial muscle formation at stage 14, *ab* mRNA can be detected in the somatic muscle cells. By stage 16, all 30 abdominal muscles ex-

press Ab, and staining with the Ab antisera indicates that all muscle nuclei express Ab (Fig. 4D). Although quantitative analysis is complicated by the adjacent epidermal staining, it is apparent that the levels of Ab in individual muscles varies. The highest concentrations are seen in the ventral longitudinal (7, 6, 13, and 12), ventral oblique (15, 16, and 17), and segmental border (8) muscles. Interestingly, the ventral longitudinal muscles are the ones that display the connectivity defects observed in *ab* mutants.

Postembryonic expression

Ab is expressed in all of the imaginal discs, a result consistent with the panoply of adult defects observed in *ab* mutants. The expression in each disc is generally strong and dispersed as shown in the eye–antennal disc (Fig. 4G) and thoracic wing–notum disc (Fig. 4H). Expression in the thoracic disc resides in regions that give rise to the scutellum and a broad section of the wing including the vein area, cell types that show defects in *ab* mutants.

ab *encodes a BTB-ZF protein*

The *ab* mRNA sequence was determined by complete sequencing of a 4.5 kb cDNA clone, pcab13 (Fig. 5). The longest open reading frame predicts a protein of 904 amino acids. The sequence surrounding the ATG codon, TTAAATGA, partially matches the consensus translation start sequence (c/aAAc/aATGG). A second in-frame ATG, located at nucleotide 171, has a perfect match (CAAAATGG) with the consensus and could serve as an alternative start codon. Sequence analysis of different cDNA clones reveals the presence of two alternatively

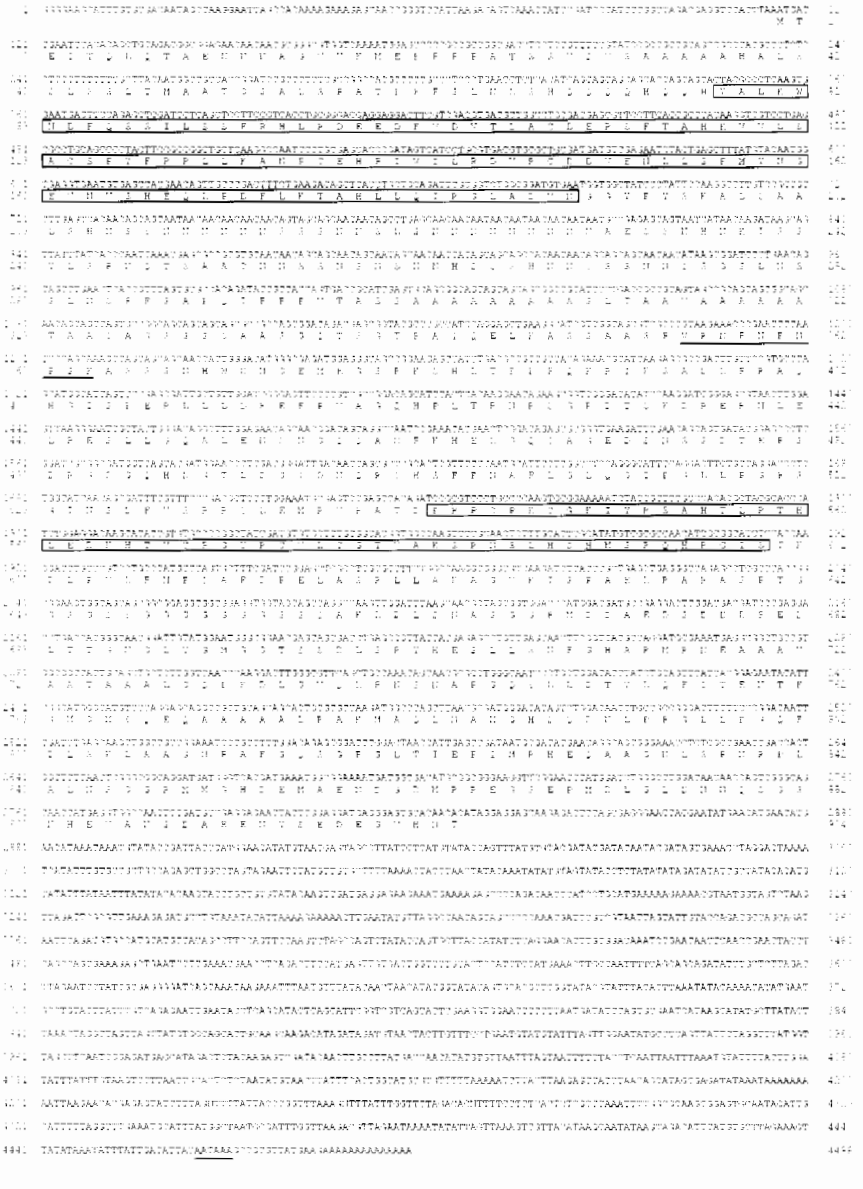

Figure 5. cDNA sequence and predicted amino acid sequence of Ab. Shown is the complete nucleotide sequence of the 4.5-kb pcab13 cDNA clone. An open reading frame of 904 amino acids is shown using the one letter code. The BTB domain is boxed (amino acid residues 78–190), and the two putative Cys_2-His_2 ZFs are also boxed (amino acid residues 543–600). The potential pcab13 polyadenylation recognition site in the 3′-untranslated region is underlined. The nucleotides 1181–1210 (underlined) are absent in several other cDNA clones and probably represent an alternatively spliced form of *ab* mRNA. The 10-amino-acid protein sequence prominently features three Asn-Pro repeats. Because sequence analysis of multiple cDNA clones and amplified PCR products provide multiple examples of each mRNA form, the difference is unlikely to be a cloning artifact. Two other cDNA clones partially sequenced were longer than pcab13 with the additional sequence attributable to longer 5′-untranslated regions.

spliced forms of *ab* mRNA. An alternative splice is used in the first exon such that different mRNAs start at the same nucleotide but are spliced either 45 bases or 93 bases downstream. In addition, embryonic mRNAs differ in the presence or absence of a 30-base insertion within the coding sequence from nucleotide position 1181 to 1210. Interestingly, this region encodes a repeated asparagine-proline motif.

The predicted Ab protein sequence belongs to the recently described family of BTB–ZF proteins (Harrison and Travers 1990; Godt et al. 1993). The Ab protein possesses two Cys_2-His_2 ZFs and a BTB domain (Figs. 5 and 6). ZFs are usually DNA-binding domains associated with transcriptional regulatory proteins, and the BTB domain is a highly conserved 115-amino-acid region, shared most often with ZF transcription factors. Staining with an Ab antisera revealed nuclear localization, consistent with a role as a transcription factor (Fig. 4D).

According to the degree of similarity between members of the BTB family, they can be subdivided into two groups: a high identity group, which includes Ab, and a low identity group (Fig. 7; Zollman et al. 1994). The high-identity group is comprised of more than a dozen *Drosophila* genes including *Broad-Complex* (*BR-C*), *ttk*, *bric-a-brac* (*bab*), *longitudinals lacking* (*lola*), and *tritho-rax-like* (*trl*). The average identity within the high-identity group is 50%. Other BTB domains are more distantly related; average identity between the two groups and among other BTB domains is 24%–30%. *Drosophila kelch*, human *LAZ3*, murine *ZF5*, and a number of poxvirus genes fall into this group. Within the BTB domain family, Ab falls into the high-identity group and its BTB domain is most closely related to *BR-C*, with 59% identity. Ab is 54% identical with Bab, 48% with Ttk, 50% with GAGA, and 47% with Lola. With lower average identity, Ab is related to ZF5 (31%), Kelch (28%), and LAZ3 (27%).

Molecular analysis of ab *mutations*

We used Southern blot analysis and PCR to map deficiency breakpoints in the region of the *ab* gene. The PCR approach involved creating primer pairs from sequenced regions of genomic DNA and cDNA clones and performing PCR on individual homozygous mutant embryos (Fig. 3). Analysis of two mutants (ab^{1D} and ab^{G5}) indicated that they were deficient for portions of the *ab* gene (Fig. 3). All of the PCR primer pairs except pair 5 failed to amplify DNA from ab^{G5} mutant embryos indicating that ab^{G5} is a deletion of at least 26 kb of DNA. Because the deletion removes coding sequences and the probable start site of transcription, ab^{G5} is predicted to be genetically null for *ab*. However, the upstream breakpoint remains unknown, and it is possible that ab^{G5} removes additional genes on chromosome 2.

In contrast, ab^{1D}, is likely to be a null, single gene *ab* mutation. This mutation was generated by transposase-induced P-element excision. Analysis of ab^{1D} indicates that the original P-element has reinserted at the same site in an inverted orientation and that an adjacent 0.7-kb deletion was generated. This deletion begins at the *P[94]* insertion site and extends 0.5 kb past the first intron, thus removing exon 1. Given the location of the ab^{1D} deletion, it is unlikely that it uncovers additional genes. Both strains were analyzed for the presence of *ab* transcripts and Ab protein by whole-mount embryo in situ hybridization and antibody staining. The results showed that one quarter of the embryos derived from heterozygous crosses lacked *ab* transcripts and protein, consistent with these *ab* mutants being null (Fig. 4F).

Portions of the *ab* gene of the EMS-induced mutations ab^{clu1} and ab^{clu2} were sequenced using a single-embryo reverse transcription–PCR method (Fig. 6). The ab^{clu2} gene contains a single nucleotide pair change (CGC to TGC) in the region encoding the second ZF, resulting in an amino acid substitution of arginine to cysteine. The presence of the novel cysteine could conceivably interfere with the structure of the ZF, which depends on its structure and function by the coordination of Zn^{+2} between cysteine and histidine residues. The ab^{clu1} mutation has a nonsense mutation (CGA to TGA; arginine to stop) 12 amino acids before the ZF and is predicted to generate a protein unable to bind DNA. These results prove that the BTB–ZF gene described here encodes the *ab* locus. Moreover, they suggest that the zinc fingers are required for normal *ab* function.

Discussion

ab *encodes a BTB–ZF transcription factor*

We have shown here that the *ab* gene encodes a BTB–ZF transcription factor by deficiency breakpoint mapping of

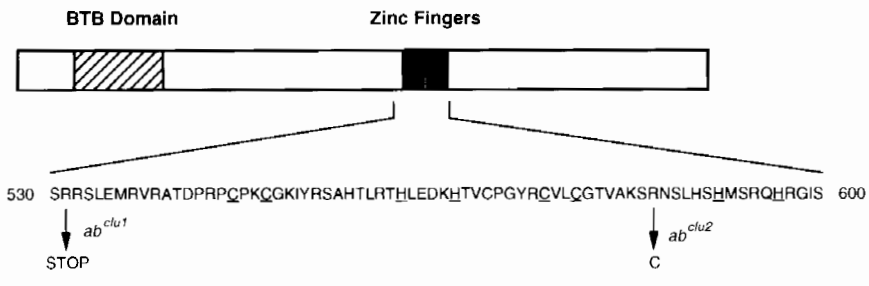

Figure 6. Sequence structure of the Ab protein and location of *ab* mutations. Shown is a boxed representation of the Ab protein, which is 904 amino acids in length. The amino terminus is shown at *left*, and amino acid residue numbering is shown at the *bottom*. (■) Two Cys_2-His_2 ZFs (amino acid residues 543–600) with their amino acid sequence shown below. The consensus ZF motif is X_3-Cys-X_{2-4}-Cys-X_{12}-His-X_{3-4}-His-X_4, and the essential Cys and His residues are underlined. The ab^{clu1} mutation introduces a termination codon at residue 531 predicting a truncated protein lacking the ZF DNA-binding domain. The ab^{clu2} mutation changes Arg585 in the second ZF to a Cys residue.

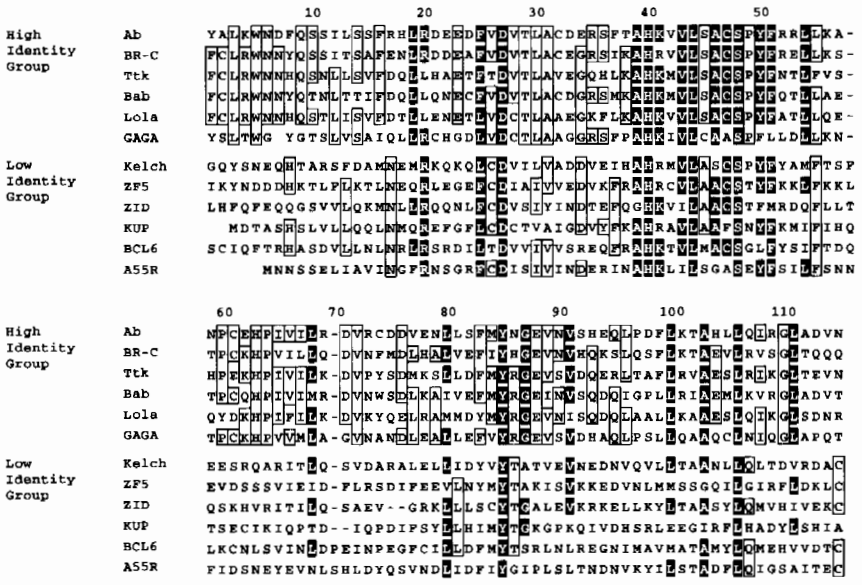

Figure 7. BTB domain sequence identities. BTB domain sequences were aligned using the Sequence Alignment program in GeneWorks (IntelliGenetics Inc.). Shown are Ab and a representative group of BTB-containing proteins, not the entire family. BTB proteins are subdivided into two groups on the basis of their degree of sequence identity: a high-identity group and a more distantly related low-identity group. Sequences are shown using the single letter code. White letters with a black background indicate those residues that are highly conserved in both groups. Black letters contained within a box indicate those residues that are conserved in only one of the two groups. Proteins listed are: Abrupt (Ab), Broad-Complex (BR-C), Tramtrak (Ttk), Bric-a-brac (Bab), Longitudinals Lacking (Lola), Kelch, and GAGA Factor (GAGA) (all *Drosophila*), murine ZF5, human ZID, KUP, and BCL6 (LAZ3), and the vaccinia virus protein A55R.

the ab^{1D} allele (induced by P-element excision) and sequence analysis of two EMS alleles. The ab^{1D} allele is transcript null and removes 0.7 kb of DNA including the first exon. The ab^{clu2} mutation has a missense amino acid substitution in the second ZF, and the ab^{clu1} allele possesses a nonsense mutation that truncates the protein and deletes the ZF.

ab *controls the specificity of neuromuscular connections*

Genetic analysis indicates that *ab* is required for SNb motor axons to recognize and synapse on their muscle targets, the ventral longitudinal muscles 7, 6, 13, and 12. The *ab* gene is expressed during the stages of motor axon outgrowth and innervation in muscle cells but not in the relevant motoneurons. This is consistent with a model in which *ab* functions within muscle cells by controlling the expression of genes involved in muscle recognition by nerve cells. Although the connectivity phenotype is most easily explained owing to lack of *ab* expression in muscles, it remains possible that the loss of *ab* CNS midline or epidermal expression results in the connectivity phenotype. This issue can be resolved by using phenotypic rescue with *ab* mutant fly strains that express *ab* specifically in the different cell types (Brand and Perrimon 1993). Because the recognition events between several motoneurons and muscles are affected, it is probable that several distinct genes involved in the recognition process may be regulated by *ab*. Muscle cell formation, differentiation, and identity are normal in *ab* mutants, with the exception of muscle attachment defects in a few muscles (see below). This result implies that the function of *ab* is not as a regulator of the initial steps of muscle development, differentiation, or identity per se but rather as a regulator operating downstream in the hierarchy and controlling the expression of muscle genes that encode specific surface or secreted proteins.

One surprising feature of *ab* expression is that it is present in the nuclei of all somatic muscle cells, not just the ventral longitudinal muscles that show the altered connectivity in *ab* mutants. Thus, it remains unclear how the restriction of *ab* function to the ventral longitudinal muscles is generated. Several explanations are possible. The *ab* gene may function in a concentration-dependent mode such that different concentrations exert different effects on gene transcription. Ab has the ability to form multimers, both in homotypic and heterotypic modes (S.H. and S.T. Crews, unpubl.), and this may be relevant because different concentrations of Ab could result in functionally different monomeric or multimeric configurations. Interestingly, *ab* is expressed at higher levels in the ventral muscle group than the lateral and dorsal groups, although the significance remains ambiguous because high levels are present in both the ventral longitiudinal muscles that show connectivity defects and the ventral oblique muscles that do not. Preliminary analysis of adult *ab* phenotypes indicate that penetrance and expressivity are sensitive to *ab* gene dosage. Dosage dependency has been observed for other BTB proteins. The *bab* gene is expressed as a gradient along the limb proximal–distal axis, and *bab* mutations result in homeotic transformations of the tarsus in a dosage-dependent fashion (Godt et al. 1993). GAGA protein can also distinguish high- and low-affinity DNA-binding sites in a concentration-dependent manner (O'Brien et al. 1995).

Spatial restriction of *ab* function could also arise through combinatorial interactions between *ab* and other transcription factors. The BTB domain of other proteins is capable of influencing protein–protein interactions as well as other functions (Bardwell and Treisman 1994). Interactions with non-BTB–ZF transcription

factors mediated by other regions of the proteins are also possible. It is estimated that the BTB–ZF protein family contains at least 40 *Drosophila* members, only a few of which have been identified (Zollman et al. 1994). It is possible that multiple BTB–ZF proteins act in concert to define regional muscle specificity by selectively regulating the expression of appropriate genes. One candidate might be the *Drosophila* (*lola*) gene. This gene encodes a BTB–ZF protein related to Ab and is expressed in muscle cells as well as the nervous system (Giniger et al. 1994). Phenotypes of *lola* mutants are complex, showing effects on axonal growth and guidance (Seeger et al. 1993; Giniger et al. 1994). Another BTB–ZF protein is Ttk that shows absence of all thoracic sensory cell bristles in null mutant mosaic patches (Salzburg et al. 1994; Guo et al. 1995). Interestingly, ab^1 and certain *ab* allelic combinations show a reduction in thoracic bristles.

Null mutations of *ab* revealed a spheroidal muscle defect in the dorsal muscles. During stage 17, muscle 1, and to a lesser extent muscle 2, was observed to pull away from its attachment site and form a spheroidal mass, a phenotype reminiscent of, but less severe than, *myospheroid* and *masquerade* mutations (Wright 1960; MacKrell et al. 1988; Murugasu-Oei et al. 1995). The establishment and maintenance of muscle attachment require proper development of muscles, extracellular matrix, and specialized epidermal segment border cells (Bate 1990; Volk and VijayRaghavan 1994). Because Ab is present in both muscle and segmental epidermal border cells, it cannot be presently determined in which cell type *ab* function is required with regards to muscle attachment.

The *ab* muscle attachment defect poses a question concerning whether the *ab* motoneuron connectivity phenotype is a secondary defect. Two lines of evidence suggest it is not. First, the embryonic muscle domains in which the two defects occur do not overlap. The spheroidal and attachment muscle defects are observed in the dorsal and lateral muscles, whereas the motoneuron connectivity defect is restricted to the ventral muscle field. Second, the EMS-induced allele ab^{clu1} has a motoneuron connectivity phenotype identical to null *ab* alleles but does not show a spheroidal muscle defect. Thus, it is likely that the connectivity and spheroidal muscle defects reflect two independent functions of *ab*, only one of which is disrupted in ab^{clu1} mutant embryos.

Properties of the ab *transcription factor*

The presence of two Cys_2-His_2 ZFs in the Ab conceptual protein sequence suggests that Ab functions as a DNA-binding transcriptional regulatory protein. This role is reinforced by the observation that Ab is localized to embryonic cell nuclei when stained with an Ab antibody. Observations made by Kalionis and O'Farrell (1993; B. Kalionis, pers. comm.) further show that Ab binds DNA in vitro. They independently cloned the *ab* gene (BK28) in a screen for *Drosophila* proteins that recognize the consensus binding sequence of the homeo domain protein Engrailed (En) (Kalionis and O'Farrell 1993). The Ab ZF binds variants of the En binding site with a slightly different preference from that of En. The similarity of the binding site of Ab and that of homeo domain proteins raises the possibility that Ab may compete or combine with homeo box-containing proteins to regulate muscle gene expression.

BTB–ZF proteins are required for a wide range of developmental events. They can be either transcriptional activators or repressors. Ttk is a transcriptional repressor of segmentation genes (Brown et al. 1991; Brown and Wu 1993; Xiong and Montell 1993). ZF5 is a mammalian transcriptional repressor of the c-*myc* protooncogene, a property that maps to the amino-terminal 279 amino acids containing the BTB domain (Numoto et al. 1993). Other in vitro experiments have shown that the BTB domain from ZID, Ttk, and GAGA inhibits the DNA-binding activity of their ZFs, as well as heterologous DNA-binding motifs, including POU–homeo domain, MADS domain, and Cys_2-Cys_2 ZFs (Bardwell and Treisman 1994). The GAGA factor acts as an activator of *Krüppel* and *Ubx* transcription through an antirepression mechanism (Kerrigan et al. 1991). *BR-C* genetically activates and represses different aspects of the ecdysone response during metamorphosis. It is unknown whether Ab acts as a transcriptional activator or repressor. Proper motor axon guidance and connectivity require not only the presence of attractive molecules, but also the absence of repulsive factors (Nose et al. 1994; Chiba et al. 1995; Matthes et al. 1995). Thus, Ab may function by activation or repression or both. Future genetic experiments are required to identify the gene targets of *ab*.

Recent evidence has suggested that BTB-containing proteins may influence transcription by modulating chromatin structure. Two BTB protein encoding genes, *Trl* and *E(var)3-93D*, are enhancers of position-effect variegation, suggesting a role in chromatin condensation (Farkas et al. 1994). GAGA factor is associated with specific regions of heterochromatin and generates nucleosome-free promoter regions both in vitro and in vivo (Raff et al. 1994; Tsukiyama et al. 1994). On the promoter of the *Drosophila hsp70* gene, GAGA proteins occupy high-affinity binding sites prior to heat shock. Upon heat shock induction, the distribution of GAGA protein spreads over the length of the transcript in a 5′ to 3′ manner, probably owing to the binding of GAGA protein to its low-affinity binding sites. The recruitment of GAGA protein to *hsp70* displays a similar kinetics to that of RNA polymerase (O'Brien et al. 1995). Because BTB domains mediate protein–protein interactions, they may interact with chromosomal complexes to open and maintain chromatin structure or interact with additional transcription factors to control transcriptional activity.

Materials and methods

Drosophila *stocks*

The ab^1 strain was acquired from the Bloomington Stock Center (Indiana University, Bloomington, IN). The BL97 enhancer trap line was created in a large-scale screen done at UCLA (Crews et al. 1992). The 94 enhancer trap line was generated

using plwB as an enhancer trap detector in the labs of Jose Campos-Ortega and Elisabeth Knust. The ab^{clu1} mutation was isolated originally in a motoneuron connectivity and guidance screen (Van Vactor et al. 1993). The following *ab* lethal mutations were generated in this study: (1) ab^{clu2} and ab^{clu3} are EMS-induced alleles identified by their failure to complement ab^{clu1} lethality, (2) ab^{60M} was generated as a homozygous lethal mutation by P-element-mediated excision of *P[BL97]* using *P[ry⁺; (Δ2-3)]* 99B as a source of transposase, (3) ab^{1D} was recovered by P-element-mediated excision/local hopping of P[94], based on its severe wing venation defect when crossed in *trans* to *P[94]*, and (4) ab^{G5} and ab^{G9} were isolated from the 94 strain as w^- revertants from progeny of 94 males irradiated with 4–6 krad of ^{60}Co. Chromosomes bearing lethal mutations were maintained as *CyO*, *CyO P[w⁺; actin5C-lacZ]*, or *CyO P[ry⁺; ftz-lacZ]* balanced stocks.

Molecular analysis of ab *gene*

Genomic DNA corresponding to the *ab* gene was initially isolated by cloning DNA adjacent to the BL97 P element. Inverse PCR (Ochman et al. 1988) was performed on BL97 DNA using primers corresponding to the 3′ end of the P element. Wild-type *Drosophila* Canton-S genomic DNA cloned into the λJ1 bacteriophage vector (constructed by S.T. Crews) was screened using ^{32}P-labeled PCR product to isolate overlapping genomic clones. Genomic DNA was extended with a chromosomal walk by screening a λfixII *Drosophila* Canton-S genomic library (Stratagene) using a *Hin*dIII–*Eco*RI genomic DNA fragment located at fragment f (Fig. 3). The DNA walking probe was labeled with digoxygenin (DIG) dUTP, and hybridization was detected using anti-DIG–alkaline phosphatase (1:10,000) and the chemiluminescent substrate Lumigen PPD (Genius system, Boehringer Mannheim).

Three *ab* cDNA clones were isolated from an embryonic 9- to 12-hr λgt11 library (constructed by Kai Zinn, California Institute of Technology, Pasadena) using radioactively labeled genomic DNA probe d (Fig. 3). The three clones (λcab1, λcab2, and λcab3) contained a common 0.6-kb *Bam*HI restriction fragment, and this fragment was radioactively labeled and used to isolate 15 cDNA clones (pcab series) from embryonic 4- to 8-hr cDNA cloned into a pNB40 plasmid library (Brown and Kafatos 1988). Clones pcab7, pcab13, pcab14, pcab26, and λcab3 were subjected to DNA sequencing. Nested deletion series were generated with exonuclease III (ExoIII) (Promega Erase-a-base Kit) on both strands and sequenced using [^{35}S]dATP on a double-stranded template (U.S. Biochemical Sequenase kit). Additional primers corresponding to the *ab* sequence were synthesized and used to complete the DNA sequence where required.

Analysis of *ab* embryonic transcripts was determined by Northern blot analysis. Samples containing 2 μg of embryonic 6- to 9-hr poly(A)$^+$ RNA were fractionated on an 0.7% /2.2 M formaldehyde–agarose gel, blotted onto a Nytran membrane, and hybridized with a ^{32}P-labeled 0.6-kb *Bam*HI *ab* cDNA fragment.

Generation of Ab antibody

Ab protein for immunization was synthesized in bacteria fused to a 6× histidine tag. The fusion genes were constructed by inserting a 681-bp *Bam*HI fragment (encoding amino acids 53–279, containing the BTB domain) and a 661-bp *Bam*HI–*Nsi*I fragment (encoding amino acids 278–498) of the *ab* cDNA into the *Bam*HI site and the *Bam*HI–*Pst*I sites, respectively, of the pQE-30 plasmid (Qiagen). Fusion proteins were prepared under denaturing conditions using Ni-NTA resin following the manufacturers recommendations (Qiagen). For immunization of rats, ~100 μg of protein was emulsified in RIBI adjuvant (Immunochem Research). Rats were injected at 2-week intervals. One week after the fourth and subsequent injections, the serum was collected and used for analysis. Prior to use, the antisera were preadsorbed against 0- to 4-hr embryos, which do not show detectable *ab* transcripts. Antisera generated using both fusion proteins gave identical staining patterns.

Antibody staining

Embryos were collected, fixed, and stained as described previously (Patel et al. 1987; Van Vactor et al. 1993). Primary antibodies were incubated with embryos at 25°C for 1 hr or overnight at 4°C. Antibodies were used at the following dilutions: monoclonal anti-β-galactosidase (Promega) at 1:500, monoclonal 1D4 anti-Fasciclin II at 1:8, anti-myosin at 1:500, and Ab antisera at 1:200. Stained whole-mount embryos were mounted in 100% methylsalicylate. Muscle staining was visualized in stage 15 to stage 17 embryos that were dissected with tungsten needles and mounted in 80% glycerol/PBS. Embryos were visualized and photographed with a Zeiss Axiophot microscope.

Polytene chromosome and embryonic whole-mount in situ hybridization

Hybridization of DNA probes to polytene chromosomes was carried out according to Langer-Safer et al. (1982). Salivary glands were dissected from third instar larvae in saline, fixed, and hybridized to biotin-dUTP-labeled DNA fragments at 42°C. Hybridization was detected using HRP-conjugated streptavidin and diaminobenzidine.

Embryo whole-mount in situ hybridization experiments were performed according to Tautz and Pfeiffle (1989). Hybridizations were carried out at 48°C for DNA probes or at 60°C for RNA probes. DIG-labeled DNA and RNA probes were labeled according to the manufacturer (Boehringer Mannheim). Hybridization was visualized by incubating hybridized and washed embryos for 2 hr with anti-DIG–alkaline phosphatase (1:2000), followed by an X-phosphate/PBT reaction. Embryos were examined and photographed as whole mounts or filets in 80% glycerol/phosphate-buffered saline (PBS).

Mapping chromosomal deficiencies by Southern blot hybridization and single-embryo PCR

Breakpoints of chromosomal deficiencies within the *ab* gene region were determined by Southern blot hybridization and single-embryo PCR. The PCR procedure utilizes primer pairs to amplify discrete genomic DNA regions, followed by gel electrophoresis to determine whether the amplified fragments are present in mutant embryo DNA. Primer pairs were designed using genomic and cDNA sequence information. Lethal *ab* deletion mutations were maintained over a *CyO* or *CyO P[ftz/lacZ]* balancer. Heterozygous flies were allowed to lay eggs, and 12 embryos were randomly picked and crushed in 5- to 20-μl lysis buffer (10 mM Tris-HCl at pH 8.0, 25 mM NaCl, 1 mM EDTA, 200 μg/ml of proteinase K). After incubation for 30 min at 37°C, the proteinase K was inactivated at 95°C for 3 min. One microliter of the embryonic DNA sample was added to 15 μl of PCR mix (Perkin-Elmer) and subjected to PCR amplification in a Perkin-Elmer 480 thermal cycler. Typical PCR parameters were 30 cycles at 94°C for 30 sec, 55°C for 45 sec, and 72°C for 90 sec followed by 1% agarose gel electrophoresis. The sample contained the primer pair from the *ab* locus and a control primer pair derived from an unlinked gene, *midway* (S. Hu and

S. Crews, unpubl.). The presence of the *midway* PCR product ensures the quality of DNA and efficiency of the PCR reaction. Presence or absence of the *ab* fragment in such mutant embryos indicates whether one or both primer sites is deleted in the mutant.

Southern blot analysis utilized restriction-cut DNA from heterozygous deletion flies that was electrophoresed and blotted onto nitrocellulose. Blots were hybridized to hexamer-primed ^{32}P-labeled DNA probes. Standard hybridization and washing conditions were used.

Sequence analysis of ab *mutants using reverse transcription (RT)–PCR*

Embryos were collected from mutant stocks balanced over *CyO P[w$^+$; actin5C-lacZ]*. Embryos were dechorionated in 50% bleach, rinsed, then rapidly transferred to heptane and cracked from their vitelline membranes by adding methanol and shaking. Embryos were rinsed with methanol, rinsed extensively with PBT, then transferred to X-gal staining solution and allowed to develop until embryos that do not have β-galactosidase activity (homozygous mutant embryos) were unambiguously discernible. Ten to twenty homozygous mutant embryos were homogenized in 0.7 ml of GHCl buffer (7.5 M guanidinium HCl, 0.025 M NaOAc at pH 7.0, 5 mM DTT, 0.5% Sarcosine, 0.5% DEPC) using a polytron homogenizer, extracted once with phenol/chloroform, then precipitated by adding 14 μl of 1 M acetic acid and 350 μl of EtOH. Pellets were resuspended in 200 μl of GHCl buffer and reprecipitated under the same conditions. Pellets were washed with 70% EtOH and resuspended in 20 μl of reverse transcriptase reaction buffer (50 mM Tris at pH 8.3, 75 mM KCl, 3 mM $MgCl_2$, 1 mM each dATP, dCTP, dGTP, dTTP, 5 mM DTT, 0.1 mg/ml of BSA, 0.5 mM primer) with 30 units of RNasin (Promega) and 200 units of Moloney murine leukemia virus (Mo-MLV) reverse transcriptase (GIBCO BRL). Reactions were incubated at 37°C for 30 min and then precipitated with 2 μl of 3 M NaOAc and 60 μl of EtOH. Pellets were resuspended directly in 50 μl of PCR amplification reaction buffer, amplified for 35 cycles at 94°C for 25 sec, 60°C for 30 sec, and 72°C for 120 sec in a GeneAmp 9600 (Perkin-Elmer), and then subjected to electrophoresis in 1% low-melting agarose. Amplification products were subcloned into *Sma*I-cut alkaline phosphatase-treated pBluescript (Stratagene). Clones were sequenced by the dideoxy chain termination method using fluorescently labeled primers and electrophoresis in an A.L.F. DNA sequencer (Pharmacia).

The primers used for RT were CTGTGGCGCACTAAACGG, AAACTGGTATACATGAGGATAAGGC, and CGCTAGCGTTGCTTAAATCC. Primers used for PCR were the same as those used for RT plus CCGGGTCCATTAAGACAGTC, GATGGAACCCTCGACGG, and TTATCACCCAATCAAACGAGC.

Acknowledgments

We thank Kayan Paydar for technical assistance; Elizabeth Knüst, Jose Campos-Ortega, and Ulrich Tepass for the 94 enhancer trap line; Frank Laski, Wei Chen, and Susan Zollman for sharing unpublished results; Bill Kalionis for communicating unpublished results regarding the BK28 gene; Dan Kiehart for anti-myosin antibody; Kai Zinn and Nick Brown for cDNA libraries; and the Bloomington Stock Center for *Drosophila* stocks. J.R.A. was supported by a National Research Service Award training grant (NS07166). This work was supported by grants from the Lucille P. Markey Charitable Trust and the National Institutes of Health (HD25251) to S.T.C. D.F. is a predoctoral fellow and C.S.G. is an investigator with the Howard Hughes Medical Institute.

The publication costs of this article were defrayed in part by payment of page charges. This article must therefore be hereby marked "advertisement" in accordance with 18 USC section 1734 solely to indicate this fact.

Note added in proof

The *ab* nucleotide sequence has been submitted to the GenBank data library.

References

Bardwell, V.J. and R. Treisman. 1994. The POZ domain: A conserved protein–protein interaction motif. *Genes & Dev.* **8:** 1664-1677.

Bate, M. 1990. The embryonic development of larval muscles in *Drosophila*. *Development* **110:** 790–804.

———. 1993. The mesoderm and its derivatives. In *Development of Drosophila melanogaster* (ed. M. Bate and A. Martinez Arrias), Vol. II, pp. 1013–1090. Cold Spring Harbor Laboratory Press, Cold Spring Harbor, New York.

Bourgouin, C., S.E. Lundgren, and J.B. Thomas. 1992. *apterous* is a *Drosophila* LIM domain gene required for the development of a subset of embryonic muscles. *Neuron* **9:** 549–561.

Brand, A.H. and N. Perrimon. 1993. Targeted gene expression as a means of altering cell fates and generating dominant phenotypes. *Development* **118:** 401–415.

Brown, H.B. and F.C. Kafatos. 1988. Functional cDNA libraries from *Drosophila* embryos. *J. Mol. Biol.* **203:** 425–437.

Brown, J.L. and C. Wu. 1993. Repression of *Drosophila* pair rule segmentation genes by ectopic expression of tramtrack. *Development* **117:** 45–58.

Brown, J.L., S. Sonoda, H. Ueda, M.P. Scott, and C. Wu. 1991. Repression of the *Drosophila fushi tarazu* (*ftz*) segmentation gene. *EMBO J.* **10:** 665–674.

Chiba, A., P. Snow, H. Keshishian, and Y. Hotta. 1995. Fasciclin III as a synaptic target recognition molecule in Drosophila. *Nature* **374:** 166–168.

Crews S., R. Franks, S. Hu, B. Matthews, and J. Nambu. 1992. The *Drosophila single-minded* gene and the molecular genetics of CNS midline development. *J. Exp. Zool.* **261/3:** 234–244.

Dohrmann, C., N. Azpiazu, and M. Frasch. 1990. A new *Drosophila* homeo box gene is expressed in mesodermal precursor cells of distinct muscles during embryogenesis. *Genes & Dev.* **4:** 2098–2111.

Farkas, G., J. Gausz, M. Galloni, G. Reuter, H. Gyurkovics, and F. Karch. 1994. The *Trithorax-like* gene encodes the *Drosophila* GAGA factor. *Nature* **371:** 806–808.

Giniger, E., K. Tietje, L.Y. Jan, and Y.N. Jan. 1994. *lola* encodes a putative transcription factor required for axon growth and guidance in *Drosophila*. *Development* **120:** 1385–1398.

Godt, D., J.L. Couderc, S.E. Cramton, and F.A. Laski. 1993. Pattern formation in the limbs of *Drosophila*: *bric à brac* is expressed in both a gradient and a wave-like pattern and is required for specification and proper segmentation of the tarsus. *Development* **119:** 799–812.

Guo, M., E. Bier, L.Y. Jan, and Y.N. Jan. 1995. *tramtrack* acts downstream of *numb* to specify distinct daughter cell fates during asymmetric cell divisions in the Drosophila PNS. *Neuron* **14:** 913–925.

Halpern, M.E., A. Chiba, J. Johansen, and H. Keshishian. 1991. Growth cone behavior underlying the development of ste-

reotypic synaptic connections in Drosophila embryos. *J. Neurosci.* **11:** 3227–3238.

Harrison, S.D. and A.A. Travers. 1990. The *tramtrack* gene encodes a *Drosophila* finger protein that interacts with the *ftz* transcriptional regulatory region and shows a novel embryonic expression pattern. *EMBO J.* **9:** 207–216.

Johansen, J., M.E. Halpern, K.M. Johansen, and H. Keshishian. 1989a. Stereotypic morphology of glutamatergic synapses on identified muscle cells in *Drosophila* larvae. *J. Neurosci.* **9:** 710–725.

Johansen, J., M.E. Halpern, and H. Keshishian. 1989b. Axonal guidance and the development of muscle fiber-specific innervation in *Drosophila* embryos. *J. Neurosci.* **9:** 4318–4332.

Kalionis, B. and P.H. O'Farrell. 1993. A universal target sequence is bound *in vitro* by diverse homeodomains. *Mech. Dev.* **43:** 57–70.

Kerrigan, L.A., G.E. Croston, L.M. Lira, and J.T. Kadonaga. 1991. Sequence-specific transcriptional antirepression of the *Drosophila* Kruppel gene by the GAGA factor. *J. Biol. Chem.* **266:** 574–582.

Keshishian, H., A. Chiba, T.N. Chang, M.S. Halfon, E.W. Harkins, J. Jarecki, L. Wang, M. Anderson, S. Cash, M.E. Halpern, and J. Johansen. 1993. Cellular mechanisms governing synaptic development in *Drosophila* melanogaster. *J. Neurobiol.* **24:** 757–787.

Kolodkin, A.L., D.J. Matthes, T.P. O'Connor, N.H. Patel, A. Admon, D. Bentley, and C.S. Goodman. 1992. Fasciclin IV: Sequence, expression, and function during growth cone guidance in the grasshopper embryo. *Neuron* **9:** 831–845.

Langer-Safer, P.R., M. Levine, and D.C. Ward. 1982. Immunological method for mapping genes on *Drosophila* polytene chromosomes. *Proc. Natl. Acad. Sci.* **79:** 4381–4385.

Lindsley, D.L. and G.G. Zimm. 1992. *The genome of* Drosophila melanogaster. Academic Press, San Diego, CA.

MacKrell, A.J., B. Blumberg, S.R. Haynes, and J.H. Fessler. 1988. The lethal *myospheroid* gene of *Drosophila* encodes a membrane protein homologous to vertebrate integrin beta subunits. *Proc. Natl. Acad. Sci.* **85:** 2633–2637.

Matthes, D.J., H. Sink, A.L. Kolodkin, and C.S. Goodman. 1995. Semaphorin II can function as a selective inhibitor of specific synaptic arborizations. *Cell* **81:** 631–640.

Murugasu-Oei, B., V. Rodrigues, X. Yang, and W. Chia. 1995. Masquerade: A novel secreted serine protease-like molecule is required for somatic muscle attachment in the *Drosophila* embryo. *Genes & Dev.* **9:** 139–154.

Nose, A., V.B. Mahajan, and C.S. Goodman. 1992. Connectin: A homophilic cell adhesion molecule expressed on a subset of muscles and the motoneurons that innervate them in *Drosophila*. *Cell* **70:** 553–567.

Nose, A., M. Takeichi, and C.S. Goodman. 1994. Ectopic expression of Connectin reveals a repulsive function during growth cone guidance and synapse formation. *Neuron* **13:** 525–539.

Numoto, M., O. Niwa, J. Kaplan, K.-K. Wong, K. Merrell, K. Kamiya, K. Yanagihara, and K. Calame. 1993. Transcriptional repressor ZF5 identifies a new conserved domain in zinc finger proteins. *Nucleic Acids Res.* **21:** 3767–3775.

O'Brien, T., R.C. Wilkins, C. Giardina, and J.T. Lis. 1995. Distribution of GAGA protein on *Drosophila* genes in vivo. *Genes & Dev.* **9:** 1098–1110.

Ochman, H., A.S. Gerber, and D.L. Hartl. 1988. Genetic applications of an inverse polymerase chain reaction. *Genetics* **120:** 621–623.

Patel, N.H., P.M. Snow, and C.S. Goodman. 1987. Characterization and cloning of fasciclin III: A glycoprotein expressed on a subset of neurons and axon pathways in *Drosophila*. *Cell* **48:** 975–988.

Raff, J.W., R. Kellum, and B. Alberts. 1994. The Drosophila GAGA transcription factor is associated with specific regions of heterochromatin throughout the cell cycle. *EMBO J.* **13:** 5977–5983.

Salzburg, A., D. D'Evelyn, K. Schulze, J.-K. Lee, D. Strumpf, L. Tsai, and H. Bellen. 1994. Mutations affecting the pattern of the PNS in Drosophila reveal novel aspects of neuronal development. *Neuron* **13:** 269–287.

Seeger, M., G. Tear, D. Ferres-Marco, and C.S. Goodman. 1993. Mutations affecting growth cone guidance in *Drosophila*: Genes necessary for guidance towards or away from the midline. *Neuron* **10:** 409–426.

Sink, H. and P.M. Whitington. 1991. Location and connectivity of abdominal motoneurons in the embryo and larva of *Drosophila melanogaster*. *J. Neurobiol.* **22:** 298–311.

Tautz, D. and C. Pfeiffle. 1989. A nonradioactive *in situ* hybridization method for the localization of specific RNAs in *Drosophila* embryos reveals translational control of the segmentation gene *hunchback*. *Chromosoma* **98:** 81–85.

Tsukiyama, T., P.B. Becker, and C. Wu. 1994. ATP-dependent nucleosome disruption at a heat-shock promoter mediated by binding of GAGA transcription factor. *Nature* **367:** 525–532.

Van Vactor, D., H. Sink, D. Fambrough, R. Tsoo, and C.S. Goodman. 1993. Genes that control neuromuscular specificity in *Drosophila*. *Cell* **73:** 1137–1153.

Volk, T. and K. VijayRaghavan. 1994. A central role for epidermal segment border cells in the induction of muscle patterning in the *Drosophila* embryo. *Development* **120:** 59–70.

Wright, T.F. 1960. The phenogenetics of the embryonic mutant, *lethal myospheroid*, in *Drosophila melanogaster*. *J. Exp. Zool.* **143:** 77–99.

Xiong, W.-C. and C. Montell. 1993. *tramtrack* is a transcriptional repressor required for cell fate determination in the *Drosophila* eye. *Genes & Dev.* **7:** 1085–1096.

Zollman, S., D. Godt, G.G. Prive, J.-L. Couderc, and F.A. Laski. 1994. The BTB domain, found primarily in zinc finger proteins, defines an evolutionarily conserved family that includes several developmentally regulated genes in *Drosophila*. *Proc. Natl. Acad. Sci.* **91:** 10717–10721.